

Enhancing current-perpendicular magnetoresistance in Permalloy-based exchange-biased spin valves by increasing spin-memory loss

J. Y. Gu, S. D. Steenwyk,^{a)} A. C. Reilly,^{b)} W. Park, R. Loloee, J. Bass,^{c)} and W. P. Pratt, Jr.

Department of Physics and Astronomy, Center for Fundamental Materials Research and Center for Sensor Materials, Michigan State University, East Lansing, Michigan 48824-1116

Inserting a thin ($t^*=0.5$ or 1 nm) layer of the antiferromagnet FeMn into the “free” Permalloy (Py) layer of a sputtered, current-perpendicular exchange-biased spin valve, Nb/FeMn/Py (pinned)/Cu/Py (free)/Nb, is shown to enhance $A\Delta R$, the difference in specific resistance between the states where the magnetizations of the two Py layers are parallel and antiparallel to each other. Such an increase is taken as evidence that spin-memory loss (spin relaxation) due to the FeMn is strong, and that judicious insertion of a source of spin relaxation into a multilayer with high specific resistance contacts can enhance $A\Delta R$, the numerator of the magnetoresistance. © 2000 American Institute of Physics. [S0021-8979(00)57308-3]

Normally, one expects that increasing spin-memory loss (spin relaxation) in a magnetic multilayer will decrease the magnetoresistance (MR). But extension of current-perpendicular (CPP) Valet-Fert (VF) theory¹ predicts that the CPP-MR can increase if a thin layer of a material X that produces strong spin relaxation is properly located within a ferromagnetic (F) layer in a sample that has superconducting (S) contacts. Achieving an increase requires satisfying two conditions: (1) the spin relaxation in X (or at the X/F interface) must be strong enough, and (2) the specific resistance ($AR_{X/F}$) of the X/F interface must be smaller than that ($AR_{S/F}$) of the S/F interface. Prior studies² show that the spin-relaxation length in thick ($t_{\text{FeMn}}=8$ nm) FeMn layers is very short ($l_{sf}^{\text{FeMn}}\sim 1$ nm) and the present study gives $AR_{\text{FeMn/Py}}$ (Py=Permalloy= $\text{Ni}_{86}\text{Fe}_{14}$) = 0.6 ± 0.2 f Ω m² $\ll AR_{\text{Nb/Py}}=3.0\pm 1$ f Ω m². We describe the apparent observation of an increase in $A\Delta R$ upon inserting 0.5 and 1 nm thick layers of X=FeMn into F=Py in samples with S=Nb. Since a similar increase in $A\Delta R$ should be achievable whenever the CPP-MR is measured with high specific resistance contacts, this result has potential technological implications.

To explain this behavior, we start with a simple F/N/F sandwich (N=nonmagnetic metal) with current flowing perpendicular to the layers, uniformly through area A. The MR is then

$$\text{MR}=[AR(\text{AP})-AR(\text{P})]/AR(\text{P})=A\Delta R/AR(\text{P}), \quad (1)$$

where the intrinsic quantities are the specific resistances

(area A times resistance R) in the states with the magnetizations \mathbf{M} of the two F layers parallel (P) or antiparallel (AP) to each other.³ Hereafter, we focus upon the numerator of Eq. (1), $A\Delta R$, the change in specific resistance between AP and P states. To achieve uniform current flow, one must attach contacts to the sample. Our contacts are Nb, which superconducts at our measuring temperature of 4.2 K.

The ideal sample is then Nb/F/N/F/Nb, and the F/Nb interfaces contribute specific resistances $AR_{\text{Nb/F}}$ that we assume are independent of the direction of electron spin along (\uparrow) or opposite to (\downarrow) the local \mathbf{M} . We define F-layer and F/N interface anisotropies by the usual parameters $\beta=(\rho_F^\downarrow-\rho_F^\uparrow)/(\rho_F^\downarrow+\rho_F^\uparrow)$ and $\gamma=(AR_{\text{F/N}}^\downarrow-AR_{\text{F/N}}^\uparrow)/(AR_{\text{F/N}}^\downarrow+AR_{\text{F/N}}^\uparrow)$, where $\rho_F^{\downarrow,\uparrow}$ ($AR_{\text{F/N}}^{\downarrow,\uparrow}$) are the F-layer resistivities (F/N interface specific resistances) for spin \downarrow,\uparrow . If the spin-diffusion length in F is “infinite” (i.e., $l_{sf}^F\gg t_F$), $A\Delta R$ should be given by the two-current series-resistor model^{1,3}

$$A\Delta R=4(\beta\rho_F^*t_F+\gamma AR_{\text{F/N}}^*)^2/(2\rho_F^*t_F+\rho_N t_N+2AR_{\text{F/N}}^*+2AR_{\text{S/F}}), \quad (2)$$

with $\rho_F^*=(\rho_F^\downarrow+\rho_F^\uparrow)/4$ and similarly for $AR_{\text{F/N}}^*$.

If a thin layer of a metal X that causes complete spin relaxation at the F/X interface is placed just inside of one of the two S/F interfaces, then VF analysis gives

$$A\Delta R=4(\beta\rho_F^*t_F+\gamma AR_{\text{F/N}}^*)^2/(2\rho_F^*t_F+\rho_N t_N+2AR_{\text{F/N}}^*+AR_{\text{S/F}}+AR_{\text{X/F}}). \quad (3)$$

That is, the addition of X between the F and S layers has two separate effects. First, it adds $AR_{\text{X/F}}$ to the denominator of Eq. (3), as would be expected from the series-resistor model. But second, as a consequence of the VF generalization of the series-resistor model, complete relaxation at the X/F inter-

^{a)}Permanent address: Physics Department, Calvin College, Grand Rapids, MI 49546.

^{b)}Permanent address: Physics Department, College of William and Mary, Williamsburg, VA 23187.

^{c)}Electronic mail: bass@pa.msu.edu

face eliminates both the expected additional term $\rho_X t_X$ and the associated $AR_{S/F}$, both of which lie outside of the MR-active region now bounded by that X/F interface. If $AR_{X/F} < AR_{S/F}$, $A\Delta R$ should then increase over its value in Eq. (2). To control the AP and P states, we deposit an 8 nm thick antiferromagnetic FeMn “pinning layer” next to one of the F layers to make an exchange-biased spin valve (EBSV).⁴ This FeMn layer “pins” the \mathbf{M} of the adjacent (pinned) Py layer so that it remains fixed at magnetic fields large enough to reverse the \mathbf{M} of the other “free” Py layer that contains the thin FeMn insert.² To grow the FeMn in the structure needed for pinning, we insert a 10 nm Cu layer between the Nb and the FeMn.⁵ With Py as our F metal, our EBSV is then Nb(250)/Cu(10)/FeMn(8)/Py(12)/Cu(20)/Py(t)/FeMn(t^*)/Py(12- t)/Cu(10)/Nb(250), where the layer thicknesses are, in nm, $t^*=0.5$ or 1 nm, t is adjustable between 1 and 11 nm, and the last Cu layer minimizes the coercive field, H_c , of the free Py layer. The outer Nb layers are crossed strips 1 mm wide. Their superconductivity ensures a uniform current flow through their overlap area $A \sim 1 \text{ mm}^2$.⁶ Separate work shows that Cu layers in contact with superconducting Nb become superconducting by the proximity effect, so their presence can be mostly neglected. Further details of our sample geometry and our sputtering and measuring techniques are given elsewhere.⁶

Because the FeMn/Py interface produces very strong spin relaxation,² using FeMn as the pinning layer in our EBSVs leads to replacement of the $AR_{S/F}$ next to the FeMn pinning layer by $AR_{\text{FeMn/F}}$ in the denominators of both Eqs. (2) and (3). This replacement has only a second order effect on the difference between Eqs. (2) and (3) described above. In addition, since l_{sf}^{Py} is not infinite ($l_{sf}^{\text{Py}} = 5.5 \pm 1 \text{ nm}$),² we must fit our data numerically using equations based upon VF theory that are more complex than Eqs. (2) and (3). Moreover, while our prior studies² argued that $l_{sf}^{\text{FeMn}} \sim 1 \text{ nm}$ in 8 nm thick layers of antiferromagnetic FeMn, we did not know if spin relaxation would be as strong in very thin FeMn layers. Our new results suggest that it is. For strong spin relaxation in the thin FeMn layers, the proper comparison standard is the EBSV Nb(250)/Cu(10)/FeMn(8)/Py(12)/Cu(20)/Py(t)/Cu(10)/Nb(250).

Figure 1 compares normalized values of AR for a comparison standard with those for two more-complex EBSVs with $t^*=0.5$ or 1 nm layers inserted into the free Py layer. The most important features of Fig. 1 are that (1) the AP and P states are well defined both for the samples with $t^*=0.5$ and 1 nm and for the comparison standard, and (2) the hysteresis curves for the samples with thin FeMn inserts are asymmetric about $H=0$. These asymmetries mean that $t^*=0.5$ and 1 nm thick FeMn layers still produce some exchange bias at 4.2 K, consistent with prior results.⁷

Data such as those in Fig. 1 let us determine values of $A\Delta R$ as functions of t . The results for $t^*=0.5$ and 1 nm and for the comparison standard are shown in Fig. 2, which contains the main experimental results of this article. For a given value of t , the data for $t^*=0.5$ nm perhaps lie slightly above those for $t^*=1$ nm and both clearly lie above those for the standard. For brevity, we neglect any differences between the data for $t^*=0.5$ and 1 nm. To explain the data in Fig. 2, we

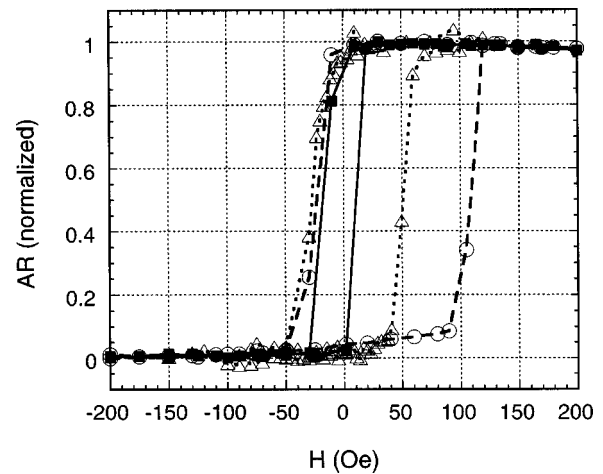


FIG. 1. Normalized AR vs H for $t=11 \text{ nm}$ for a comparison standard (closed squares and solid curve) and for $t^*=0.5 \text{ nm}$ (open triangles and dotted curve) and $t^*=1 \text{ nm}$ (open circles and dashed curve).

propose that the thin FeMn inserts produce strong spin relaxation, leading to replacement of a large value of $AR_{\text{Nb/Py}}$ in the denominator of Eq. (2) by a smaller value of $AR_{\text{FeMn/Py}}$ as in the denominator of Eq. (3).

To support this proposal, we turn to quantitative analysis. To minimize adjustability of parameters, we first predict how the data of Fig. 2 should behave using parameters we have already published for all of the constituents of the EBSVs,² with no adjustment, plus a newly measured value of $AR_{\text{FeMn/Py}} = 0.6 \pm 0.2 \text{ f}\Omega \text{ m}^2$. In Fig. 3 the broken curve represents the predictions for $A\Delta R$ for our comparison samples and the dotted curve represents the predictions for $A\Delta R$ for $t^*=1 \text{ nm}$ (if l_{sf}^{FeMn} is very short, the predictions for $t^*=0.5$ and 1 nm are the same). The positive feature of these two curves is that their difference is similar to what we observe. The negative feature is that the absolute values of the predictions in both cases miss the data—they are too small at large t and too large at small t .

In examining both our present comparison data and our previously published data for Py-based EBSVs,² we find two

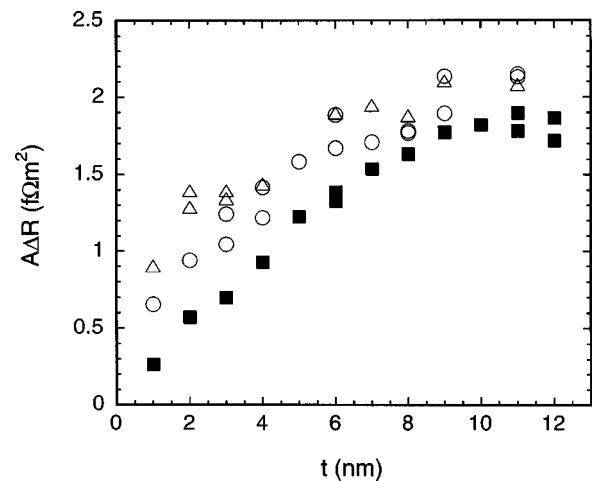


FIG. 2. $A\Delta R$ vs t for comparison standards (closed squares) and samples with $t^*=0.5 \text{ nm}$ (open triangles) and $t^*=1 \text{ nm}$ (open circles).

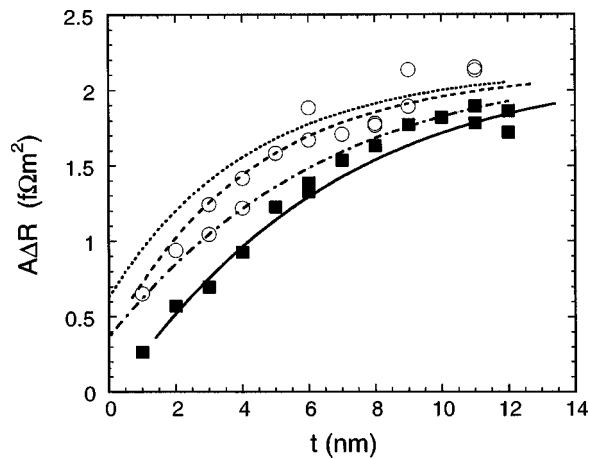


FIG. 3. Experimental data for comparison standards (closed squares) and for $t^*=1$ nm (open circles). The broken and solid curves are the initial and modified calculations for the comparison standards. The dotted and dashed curves are the initial and modified calculations for samples with $t^*=1$ nm.

sources for the difference between the prediction of the broken curve in Fig. 3 and the comparison standard data (closed squares).

First, our new comparison $A\Delta R$ data for $t=12$ nm are larger than our prior equivalent data² by $\sim 15\%$. Since taking those prior data, we have changed the argon cleaning system, the computer control program, and the masks. We now have several sets of data suggesting that our new values of $A\Delta R$ for Py-based EBSVs with thick Py layers are, on average, about 15% larger than the data in Ref. 2. A straightforward way to correct this difference is to increase our “best estimate” of $\beta=0.73$ (± 0.07) to 0.77, still well within our original estimate of uncertainty.

Second, both our prior and new data fall below prediction for very thin t ($t \leq 3$ nm). In analyzing our prior data, we neglected this “problem,” assuming that the thin layer data were less reliable due to interfacial intermixing and finite interface thickness. Because of the importance of the thin t data in the present study, we cannot neglect such data, but must find a way to treat them. Among the alternatives tried, the simplest seems to be to assume that the appropriate thickness of the Py for the analysis is less than the intended thick-

ness because of finite thickness of the interfaces—presumably alloys of Py/Cu (Ref. 8) or Py/FeMn. From other studies,⁹ interfacial thicknesses due to alloying in our sputtered samples seem to extend over a range of 0.6–0.9 nm. We can fit our comparison data in Fig. 3 by subtracting 0.7 nm from each Py layer thickness for each Py/Cu interface, including the one next to the Nb for the comparison standard. The combined effect of increasing β to 0.77 and subtracting 0.7 nm from each Py/Cu interface is shown in Fig. 3 as the solid curve for our comparison standards and as the dashed curve for the samples with $t^*=1$ nm. The parameters chosen so that the modified “predictions” fit the comparison standard also fit the data for $t^*=1$ nm rather well.

To conclude, we have shown that inserting thin ($t^*=0.5$ and 1 nm) FeMn layers into the middle of the free Py layer of a Py-based EBSV with Nb contacts leads to a larger $A\Delta R$ than that for a comparison standard. We propose that this increase is due to introduction of strong spin relaxation by the thin FeMn inserts, leading to replacement of a larger $AR_{\text{Nb/Py}}$ by a smaller $AR_{\text{FeMn/Py}}$, in analogy with the difference between Eqs. (2) and (3).

This work was supported by U.S. NSF Grant Nos. DMR 98-20135 and MRSEC 98-09688, the Michigan State University Center for Fundamental Materials Research and Center for Sensor Materials, and Ford Research Laboratories.

¹T. Valet and A. Fert, Phys. Rev. B **48**, 7099 (1993).

²W. P. Pratt, Jr., S. D. Steenwyk, S. Y. Hsu, W.-C. Chiang, A. C. Schaefer, R. Loloee, and J. Bass, IEEE Trans. Magn. **33**, 3505 (1997); S. D. Steenwyk, S. Y. Hsu, R. Loloee, J. Bass, and W. P. Pratt, Jr., J. Magn. Magn. Mater. **170**, L1 (1997).

³S. F. Lee, W. P. Pratt, Jr., Q. Yang, P. Holody, R. Loloee, P. A. Schroeder, and J. Bass, J. Magn. Magn. Mater. **118**, L1 (1993).

⁴B. Dieny, V. S. Speriosu, S. Metin, S. S. P. Parkin, B. A. Gurney, P. Baumgart, and D. R. Wilhoit, J. Appl. Phys. **69**, 4774 (1991).

⁵C. Tsang and K. Lee, J. Appl. Phys. **53**, 2605 (1982).

⁶S. F. Lee et al., Phys. Rev. B **52**, 15426 (1995).

⁷S. S. P. Parkin and V. S. Speriosu, in *Magnetic Properties of Low-Dimensional Systems II*, edited by L. M. Falicov, F. Mejia-Lira, and J. L. Moran-Lopez, Springer Proceedings in Physics, Vol. 50 (Springer, Berlin, 1990), p. 110.

⁸V. S. Speriosu, J. P. Nozieres, B. A. Gurney, B. Dieny, T. C. Huang, and H. Lefakis, Phys. Rev. B **47**, 11579 (1993).

⁹L. L. Henry, Q. Yang, W.-C. Chiang, P. Holody, R. Loloee, W. P. Pratt, Jr., and J. Bass, Phys. Rev. B **54**, 12336 (1996).